Vibrational Relaxation in Atactic Polystyrene: A Calculation of the Frequency Correlation Functions of Ring Stretching Modes and Their Variation with Temperature

Paul Painter,*,† Maria Sobkowiak,† and Yung Park‡

Materials Science and Engineering Department, Pennsylvania State University, University Park, Pennsylvania 16802, and Department of Polymer Science and Engineering, Sunchon National University, 315 Maegokdong Sunchon, Jeonnam, Korea

Received October 20, 2006; Revised Manuscript Received December 14, 2006

ABSTRACT: Time correlation functions and their variation with temperature have been calculated for the modes observed near 1601 and 1583 cm^{-1} in the infrared spectra of atactic polystyrene. The correlation functions deviate from the Kubo−Rothschild model describing the fast modulation limit but can be modeled by simply assuming that there is a fast relaxation process characterized by a single relaxation time that is inhomogeneously broadened. It is noted that as long as the relaxations associated with inhomogeneous broadening are all relatively slow processes (in terms of vibrational relaxations), then their only contribution to the band profile would be through a Gaussian term that modifies the simple Kubo−Rothschild expression. The factors that contribute to this inhomogeneous broadening are discussed. Dynamic heterogeneity presumably plays a significant role, but in addition the 1583 cm^{-1} band appears to be influenced by an anharmonic coupling to lower frequency modes that provides an additional mechanism of relaxation. As a result, this mode is particularly sensitive to temperature, displaying changes in the relaxation time and second moments that show a transition near 80 °C, about 20 °C below the thermally observed T_g.

Introduction

In studies of polymer transitions reported more than 30 years ago, it was observed that infrared band frequency shifts and intensity changes show inflection points around the T_g and the melting point.[1−4] More recently, Tashiro and Yoshioka[5] used the sensitivity of the half-width of bands in the infrared spectra of syndiotactic polystyrene to probe the crystallization process. As part of this study, these authors also monitored the peak position and half-width of the 907 cm^{-1} band of atactic polystyrene (*a*-PS) as a function of temperature, observing intriguing changes near the T_g. Following this work,[6] we studied two ring-stretching modes near 1600 cm^{-1} in the infrared spectrum of *a*-PS. It was observed that both the shape and width at half-height of one of the fundamental modes in this region of the spectrum change significantly as the polymer is heated through the glass transition temperature. This was interpreted in terms of a coupling of this mode to lattice vibrations through an overtone vibration.

It is well-known that Raman and infrared bandwidths and shapes are sensitive to vibrational relaxation processes and picosecond dynamics.[7−10] Analysis of bandwidths and band shapes has been a largely neglected topic in polymer vibrational spectroscopy, however. In part, this is because there are a number of experimental and computational problems, well documented in the literature. Nevertheless, in studies of small molecules, band contour analysis has provided information on (among other things) rotational relaxation, the duration of "sticky" collisions (e.g., hydrogen bonds), the dynamics of strong interactions, the coupling of local vibrations with lattice motions, and so on.[11−23] The continued development and application of time domain techniques still promises to yield the most detailed information on picosecond time scale relaxation phenomena, but relatively few groups are equipped to perform these sophisticated and difficult experiments. Accordingly, there is still significant insight and progress to be made through the simpler study of the shapes of infrared bands and Raman lines. Here we will consider the calculation of time correlation functions and their variation with temperature from the infrared data we presented previously.[6] Before getting to this, we will present a brief review of the factors that affect bandwidths and shapes, in order to provide a context for the subsequent discussion of our results.

Background Material: Intensity Distribution in the Vibrational Spectra of Polymers

In considering the vibrational spectra of condensed matter, we can neglect the effect of factors such as natural and Doppler broadening, Boltzmann factors, etc., which make very small contributions to the width of bands relative to other processes in the relatively limited temperature range used in most polymer studies.[24] Accordingly, the major factors that would be expected to affect the shape and intensities of infrared bands and Raman lines are (i) conformation, (ii) inhomogeneous broadening and phase relaxation, (iii) rotational relaxation, (iv) resonance energy transfer, and (v) vibrational energy relaxation.

One advantage immediately follows from studying macromolecules. Because of their large mass and moments of inertia, relaxation times associated with the reorientation of chain segments and many side groups are long compared to vibrational relaxations, and their contribution to band and line contours can be neglected.[11] However, this is accompanied by the complications introduced by sensitivity to conformation. Fortunately, in the spectra of most polymers there are modes that are largely localized. Normal-mode calculations indicate that the ring stretching modes near 1600 cm^{-1} in the vibrational spectra of *a*-PS are good examples of such conformationally insensitive bands.[25−27]

† Pennsylvania State University.
‡ Sunchon National University.

10.1021/ma062423c CCC: $37.00
Published on Web 02/09/2007

In the vibrational spectra of amorphous polymers, even modes that are insensitive to conformation are broad relative to low molecular weight liquids and display changes in intensity and shape as a function of temperature. This is usually considered a consequence of *inhomogeneous broadening*. In the disordered state, there is a distribution of local environments, and as a result, there is no longer a single transition energy, but a band. Each individual oscillator may relax by some mechanism (e.g., vibrational dephasing or energy relaxation), but the band due to a particular normal mode would then reflect a superposition of the frequencies of the individual oscillators. As we will discuss in more detail below, the widely used Kubo−Rothschild model assumes that each oscillator relaxes in an exponential fashion (hence has a Lorentzian band shape), but there is a Gaussian distribution of such modes. The term "inhomogeneous broadening" has been used in a number of contexts, however, and its meaning is related to the speed of relaxation or what is referred to as the dephasing process. In *pure phase relaxation*, even if the normal modes on each molecule in a system are excited simultaneously, because they have slightly different frequencies (as a result of interactions and small differences in local environments), they get out of phase with one another as time progresses, resulting in destructive interference. The shape and breadth of a band then depend on how fast this happens. If dephasing is fast, the effects of local differences in environment are averaged out by the rapid "loss of memory". If it is assumed that a single, fast process governs relaxation, then the resulting band shape will be Lorentzian and the relaxation time will be inversely proportional to the bandwidth. In low molecular weight liquids, for example, local interactions fluctuate rapidly as a result of the translational and rotational motion of the molecules. All the molecules then appear to be the same or very similar to the radiation field, so that a motional narrowing of the inhomogeneously broadened band is observed. On the other hand, if "modulation" is slow, the observed band shape will be Gaussian and simply reflect the distribution of local environments. Accordingly, we would expect to see a narrowing of the observed bands or lines of amorphous glassy polymers when dissolved in a solvent and perhaps similar changes as a result of going from the glassy to the melt state.

Vibrational energy can also relax by resonance transfer processes. A particularly striking example of this type of relaxation occurs in molecules containing carbonyl groups. Acetone, for example, has been widely studied.[7,28] In molecules such as this, local structure, as influenced by strong interactions between permanent dipole moments, coincides with strong vibrational coupling that is a consequence of transition dipole interactions. The former influences the latter as a result of the tendency of the molecules to align to some degree, even in the liquid state. This coupling results in an asymmetric broadening of the observed vibrational mode, in this case the carbonyl stretching vibration, as we also observed in studies of ethylene/vinyl acetate copolymers a few years ago.[29] However, *a*-PS is a nonpolar molecule, and resonance energy transfer would not be expected to play a major role in vibrational relaxation processes in this material.

Inelastic collisions can result in an energy transfer, and vibrational energy can also decay by transfer to other, lower energy modes (vibrational relaxation), whose vibrations may be coupled to the mode of interest or to overtone or combination modes that are close in frequency. Low-frequency modes can play an important and intriguing role in this process. If, for example, an overtone is separated from a fundamental by a few wavenumbers, a lattice or bath mode can "make up" the energy difference between the fundamental and the overtone, ensuring a conservation of energy and providing a mode of relaxation.[12] This would result in a sensitivity of the high-frequency mode band shapes to relaxation phenomena like the T_g. We believe we have observed a coupling of one of the ring modes of *a*-PS to a combination mode through a bath mode,[6] as mentioned in the Introduction.

Theories of Vibrational Relaxation

There are a number of models of vibrational relaxation that have been developed to describe various forms of "modulation". The most widely used of these is due to Rothschild[11] and is based on a treatment of line shapes by Kubo.[30] This model applies to what is called the fast modulation limit, where the time scale of the fluctuations (often equated to collisions) is small. The model starts with an inhomogeneously broadened band or line, where it is also assumed that local variations in environment, hence interactions, are random about a mean, so that the distribution of modes about this mean takes a Gaussian form. The second moment of a band contour, M_2, is given by

$$M_2 = \frac{\int_{-\infty}^{+\infty} I_{vib}(\omega)(\omega - \omega_0)^2 \, d\omega}{\int_{-\infty}^{+\infty} I_{vib}(\omega) \, d\omega} \tag{1}$$

where ω_0 is the band center (usually determined from the first moment). For a Gaussian process, the second moment is the familiar "random walk" result.

$$\langle \{\omega_1(t=0)\}^2 \rangle^{1/2} = \{M_2\}^{1/2} \tag{2}$$

The frequency of vibration of a particular normal mode of a molecule at an instant of time, t, is $\omega_0 + \omega_1(t)$. In other words, local interactions result in a shift of $\omega_1(t)$ from the unperturbed value, ω_0. The average of this shift over time results in a Gaussian line shape. If it is now assumed that each of the individual modes that contribute to a profile is characterized by a correlation function that decays exponentially with a correlation time τ_c, $\exp(-t/\tau_c)$, then the following expression for the vibrational time correlation function can be obtained:[11]

$$G_V(t) = \exp\{-M_2\tau_c^2[\exp(-t/\tau_c) - 1 + t/\tau_c]\} \tag{3}$$

The interesting part of this model is the behavior predicted at the limits of short and long times. In what is called the slow modulation limit, when the time scale of the fluctuations, τ_c, in the system is large, or at very short times ($t \rightarrow 0$), the time correlation function is Gaussian.

$$G_V(t) = \exp(-0.5M_2t^2) \tag{4}$$

(In order to obtain this result, put $\exp(-t/\tau_c) = 1 - t/\tau_c + t^2/2\tau_c^2$ in eq 5.) Because the time correlation function is Gaussian, its Fourier transform results in a Gaussian band shape, one that reflects the distribution of local environments and hence interactions.

In the fast modulation limit, when the time scale of the fluctuations, τ_c, in the system is small (modulation frequency $\sim 1/\tau_c$), or at very long times ($t \rightarrow \infty$), the time correlation function is exponential.

$$G_V(t) = \exp(-t/\tau_r) \tag{5}$$

where

$$\tau_r = 1/M_2\tau_c \quad (6)$$

The Fourier transform of this exponential gives a Lorentzian band shape.

A serious limitation of this model would appear to be the dependence of the correlation function on a single relaxation time. This relaxation time is presumably a sum of various contributions, including vibrational energy relaxation processes as well as pure dephasing. However, energy relaxation processes appear to be relatively slow in many of the small-molecule systems that have been studied. Accordingly, the Kubo−Rothschild model has been successfully applied to a description of vibrational relaxation in a large number of molecular liquids, particularly those where intermolecular interactions are weak. However, deviations from this simple model can be observed in various systems, particularly (but not exclusively) those involving strong interactions between the molecules (e.g., hydrogen bonds), where the phase memory is long. The infrared band or Raman line appears to be more Gaussian and is said to be inhomogeneously broadened.[31−35]

This can be confusing because inhomogeneous broadening appears to be an essential component of the Kubo−Rothschild model for fast phase relaxation through the parameter M_2, the second moment of the band. However, in this model ($\tau_c \ll 1$ ps) the correlation function (eq 3) only reflects the distribution of environments at $t \approx 0$. Accordingly, this parameter then reflects what is called *static inhomogeneous broadening*. In what follows, we will distinguish between fast and slow relaxation processes. Homogeneous broadening is then a consequence of processes that occur on a rapid time scale, where τ_c is small (or the frequency of modulation, τ_c^{-1}, is large). Inhomogeneous broadening is a result of processes that occur more slowly. The observed band is a convolution of these two effects, and the frequency correlation function can then be written as a product of two correlation functions:[31−37]

$$G_V(t) = \Phi_h(t)\,\Phi_i(t) \quad (7)$$

As George et al. pointed out,[33] this separation is only strictly valid if the homogeneous and inhomogeneous correlation functions decay on different time scales. It is usual to assume that the correlation function of the modulation is exponential so that both $\Phi_h(t)$ and $\Phi_i(t)$can be written in the same form as eq 3. The homogeneous (rapid modulation) function is then

$$\Phi_h(t) = \exp\{-\Delta\omega_h^2\tau_c^2[\exp(-t/\tau_c) - 1 + t/\tau_c]\} \quad (8)$$

$\Delta\omega_h^2$ is the contribution to the second moment of the band that is due to static inhomogeneous broadening (i.e., reflects the distribution of local environments at the moment the normal mode is excited). If it is assumed that inhomogeneous broadening is a result of processes that occur slowly (correlation time, $(\tau_c)_i$, large), then the inhomogeneous correlation function becomes Gaussian:

$$\Phi_i(t) = \exp\left\{-\frac{1}{2}\Delta\omega_i^2 t^2\right\} \quad (9)$$

The experimental M_2 is then given by

$$M_2 = \Delta\omega_h^2 + \Delta\omega_i^2 \quad (10)$$

Note that if a number of different processes contribute to inhomogeneous broadening, then as long as the correlation time of each is large, we will simply have a product of $\Phi_i(t)$ Gaussian terms in eq 7. Such a product is simply another Gaussian with a single parameter that is a sum of individual contributions ($\Delta\omega_i^2$) to the second moment, M_2. It will be shown below that eqs 7−10 provide a good to fit the data.

Calculations

In order to calculate time correlation functions from spectroscopic data, various difficulties must be overcome. First, any band-shape distortions introduced by the instrument must be taken into account. The FTIR data used in this study had a ratio of apodized resolution to full width at half-height of between 0.11 and 0.16, so band shape corrections were considered unnecessary. Second, a baseline must be correctly identified and set. We discussed the identification of the baseline at length in our preceding paper and believe it can be established with only small errors, as long as careful attention to sample preparation is paid.[6] Third, in using infrared spectroscopy, the variation of the refractive index across an absorption band must be taken into account. However, for the relatively weak modes that are the subject of this study, it has been found that the refractive index varies between values of about 1.47 and 1.49 across the band profile,[38] so corrections for this factor were neglected. Finally and most crucially, a way must be found to deal with the overlap of modes commonly found in polymer materials.

The problems of dealing with overlapping modes appear to have been successfully tackled in a number of studies of small molecules. Kirillov[23] has proposed a time domain function that has an analytical counterpart in the frequency domain and can apparently fit bands or lines that are intermediate in shape between Gaussian and Lorentzian. This correlation function reduces to Gaussian and exponential forms in a similar fashion to the Rothschild−Kubo model in the limits described above. However, we were unsuccessful in applying this model to the 1600 cm^{-1} region of the spectrum of polystyrene, either because of convergence problems in the way we were performing the calculations or (more probably, we think) because the Kirillov model needs to be modified to account for inhomogeneous broadening. Accordingly, we used a curve-resolving approach, following the work of Georgini et al.,[39] who curve-fit the −CN stretching region of the liquid crystal ME6N to three Voigt profiles to account for the fundamental mode and two weak satellite (Raman) lines. The line shape of the fundamental was then Fourier inverted to give the time correlation function.

An experimental band profile is simply a series of data points, so if a function gives an exact fit to this profile (or one that is within the precision of the data), it seems reasonable to assume that the time correlation function calculated by numerical Fourier transformation of this band is a close representation of the original data. There are various curve-fitting routines commercially available that use Voigt functions or some sort of sum of Lorentzian and Gaussian functions. In our work, the following sum function was used:

$$I(\nu) = fA_0 \exp[-\ln 2(\nu - \nu_0)/\Delta\nu_{1/2}]^2 + (1-f)A_0/\{1 + [(\nu - \nu_0)/\Delta\nu_{1/2}]^2\} \quad (11)$$

The Gaussian and Lorentzian shapes that combine to make up the overall band profile are assumed to have equal half-widths at half-height, $\Delta\nu_{1/2}$, and are present in the proportions of f to $(1-f)$. A_0 is the peak height, ν_0 is the wavenumber coordinate of the peak maximum, and ν are the frequencies of the points that describe the bands. Liu et al.[40] have recently shown that this particular sum function is an excellent approximation to a true Voigt profile, with maximum errors of width, area, and peak height of 0.01%, 0.2%, and 0.55%, respectively.

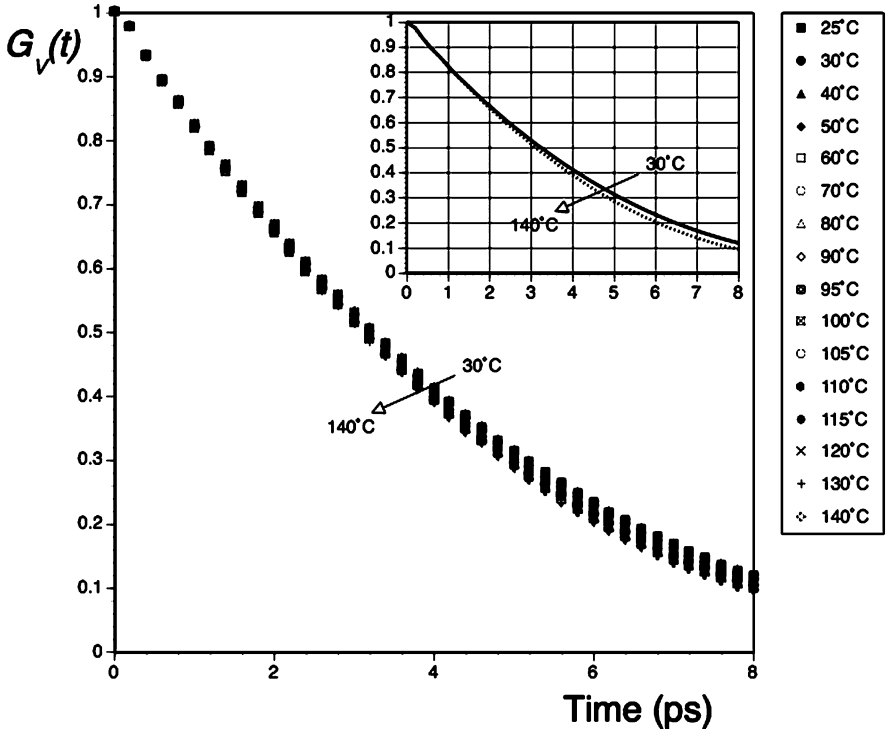

Figure 1. Plot of the time correlation functions calculated for the 1601 cm^{-1} band of *a*-PS as a function of temperature. The inset shows some selected curves to give a better view of the trends.

Accordingly, we generated bands using the parameters obtained from curve resolving; the intensity at maximum absorption (A_0), the full width at half-height ($2\ \Delta\nu_{1/2}$), and the band-shape parameter (fraction Gaussian, f), using eq 11. The frequency of each band maximum, ν_0, was set to 0 cm^{-1}. Band absorbance values were normalized to unit band area (to partially account for local fields[7]). The bands were generated out to ± 100 cm^{-1}, and the resolution of the original FTIR data was 1 cm^{-1}. Upon numerically Fourier transforming the bands (using a program written in MATLAB), this gave a frequency correlation function that, in principle, is reliable to 16 ps at a time resolution of about 0.17 ps.[7] Calculated correlation data were normalized to a value of 1 at $t = 0$.

Results and Discussion

The band shapes of both the 1601 and 1583 cm^{-1} modes of *a*-PS are neither pure Gaussian nor Lorentzian[6] and therefore do not reflect just the distribution of local oscillator environments or pure relaxation processes, but some combination of the two. The time correlation functions calculated for these bands are shown in Figures 1 and 2, respectively. For the 1601 cm^{-1} band, there are only small changes in $G_V(t)$ as the temperature is increased from 25 to 140 °C. There is slightly faster correlation decay at higher temperature, reflecting a small broadening of the band.[6] In contrast, there are large changes in $G_V(t)$ calculated for the band near 1583 cm^{-1} as a function of temperature. The correlation decay apparently becomes slower, reflecting the (small) narrowing of the bandwidth and change in band shape of this mode.[6] This difference in the behavior of the 1601 and 1583 cm^{-1} bands would seem to reflect differences observed in the ν_2 and ν_3 modes of chloroform by Rothschild and Cavagnat.[12] These authors observed that the vibrational amplitude correlation decay of the ν_2 mode was faster at higher temperature, while that of the ν_3 mode was slower. Vibrational dephasing and vibrational energy relaxation have the opposite dependence on temperature. Faster correlation decay at higher temperatures is attributed to vibrational dephasing, while slower correlation decay at higher temperatures indicates that vibrational energy relaxation occurs. At first sight, this would seem to contradict our spectroscopic observations that the 1583 cm^{-1} band changes more dramatically with temperature than the 1601 cm^{-1} band because of a coupling to a combination mode that is probably mediated by a lattice or bath mode, thus suggesting a loss of correlation due to energy relaxation.

This apparent difference is a consequence of inhomogeneous broadening in the *a*-PS ring modes studied here. This can be seen in Figures 3 and 4, where we attempted to fit the time correlation functions calculated for the 1601 and 1583 cm^{-1} modes to the Kubo−Rothschild model (eq 3). It can be seen that the calculated data deviate from this model, with the deviation increasing as the temperature is raised. The deviation of the 1583 cm^{-1} mode is far greater than that of the 1601 cm^{-1} mode. These plots indicate that there are processes occurring on (at least) two different time scales. The first is a fast process, where τ_c is small (modulation frequency $\sim 1/\tau_c$). The second is a much slower process (or processes), where τ_c is large, accounting for the deviations between the values of $G_V(t)$ calculated from spectroscopic data and the curve calculated using eq 3. Essentially, the degree of inhomogeneous broadening of the bands is changing, and this could be due to changes in both the static inhomogeneous broadening component as the polymer approaches the T_g and a contribution from a slow relaxation process.

In general, the same band shape can arise from various combinations of homogeneous, inhomogeneous, and intermediate mechanisms, making it difficult to extract information on the dynamics of the system in the absence of additional information. As mentioned above, one approach has been to assume that vibrational relaxation occurs on just two time scales, one fast and the other slow, and each of these can be modeled using an expression of the same form as eq 3.[31−37] Following this approximation, we assumed that τ_c is large for the slow relaxation process (or processes) and least-squares fit the values of $G_V(t)$ to eqs 7−9 under the constraint imposed by eq 10 (i.e.,

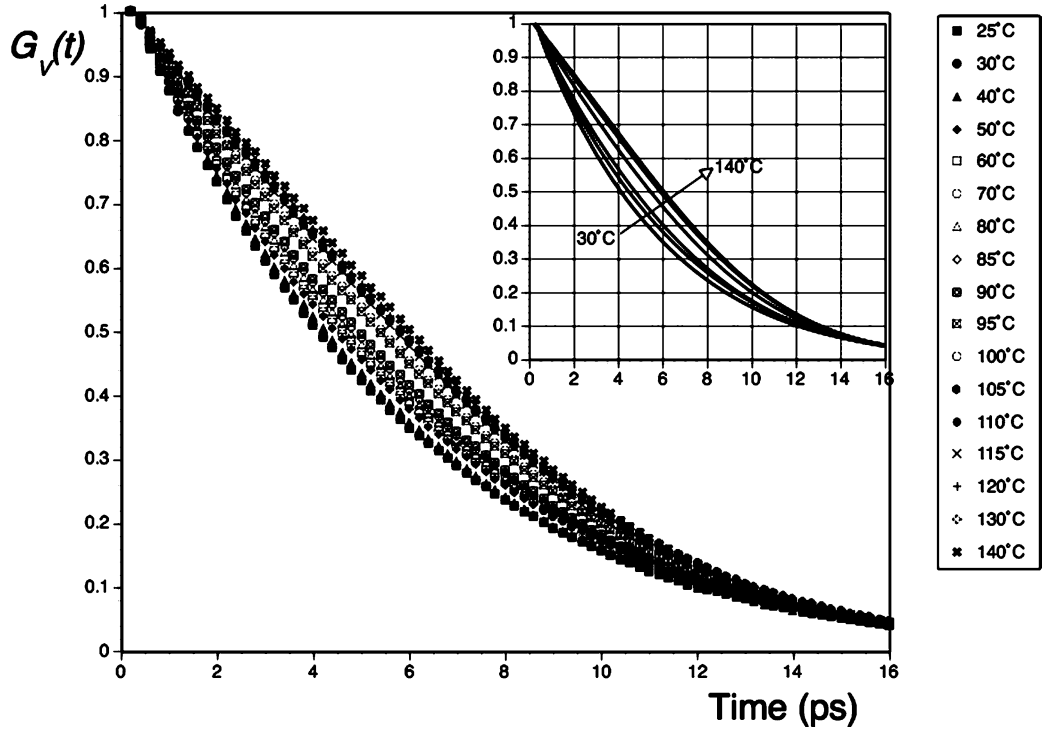

Figure 2. Plot of the time correlation functions calculated for the 1583 cm^{-1} band of *a*-PS as a function of temperature. The inset shows some selected curves to give a better view of the trends.

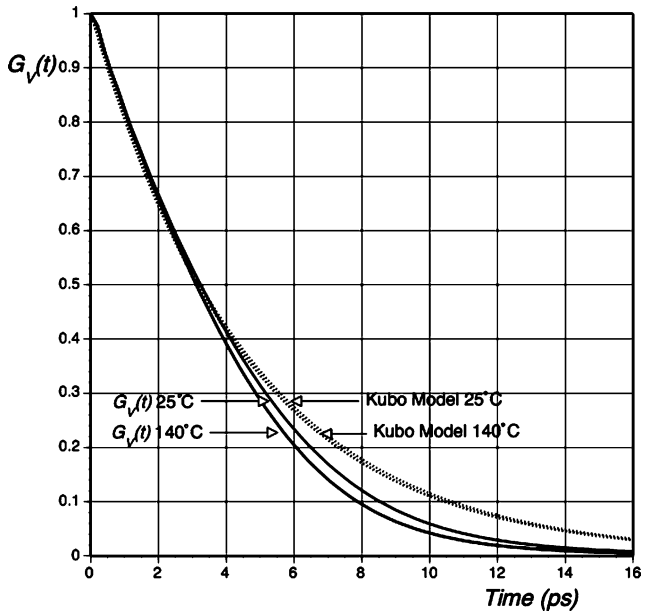

Figure 3. Plot of the time correlation functions calculated for the 1601 cm^{-1} band of *a*-PS from spectroscopic data obtained at 25 and 140 °C. Also shown are curves calculated using the Kubo model so as to give the best fit at short times.

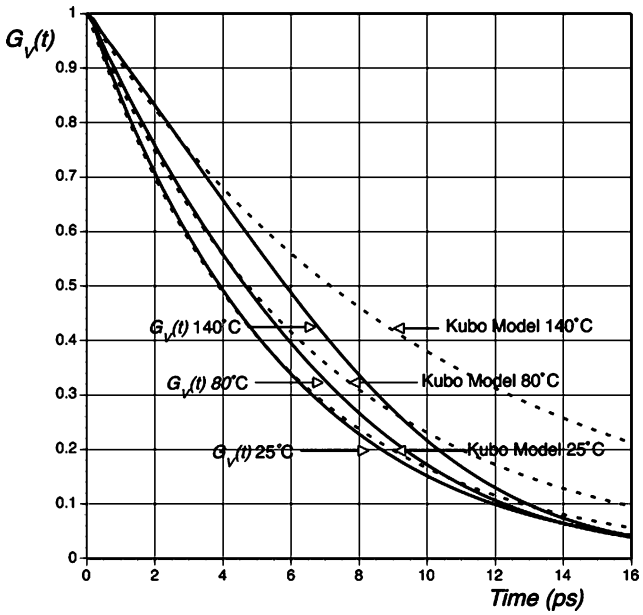

Figure 4. Plot of the time correlation functions calculated for the 1583 cm^{-1} band of *a*-PS from spectroscopic data obtained at 25, 80, and 140 °C. Also shown are curves calculated using the Kubo model so as to give the best fit at short times.

we assumed that the contributions of homogeneous and inhomogeneous broadening, $\Delta\omega_h^2$ and $\Delta\omega_i^2$, to the band profile must sum to give the experimental second moment, M_2). The results are shown in Figure 5 for the 1583 cm^{-1} mode at 25 and 140 °C. Equally good fits for the time correlation functions calculated for the 1601 cm^{-1} mode were obtained. Accordingly, even though the assumption of just two relaxation regimes, slow and fast, appears to be quite drastic and a source of error that is hard to estimate, the results we obtain fit the data and, as we will discuss below, are consistent with other work on relaxation in polymer materials.

The values of τ_c, $\Delta\omega_h^2$, and $\Delta\omega_i^2$ obtained from a fit to eqs 7−10 are shown in Figures 6, 7, and 8, respectively, while a plot of M_2 as a function of temperature is shown in Figure 9. It can be seen from Figure 7 that the fast relaxation process occurs in the subpicosecond regime, with τ_c having values of the order of 0.016 ps for both modes at 25 °C. However, the correlation time calculated from the 1601 cm^{-1} band changes only a small amount with temperature (and the variation is probably within the range of error), but τ_c for the 1583 cm^{-1} band changes much more significantly, with the relaxation time becoming faster at higher temperatures.

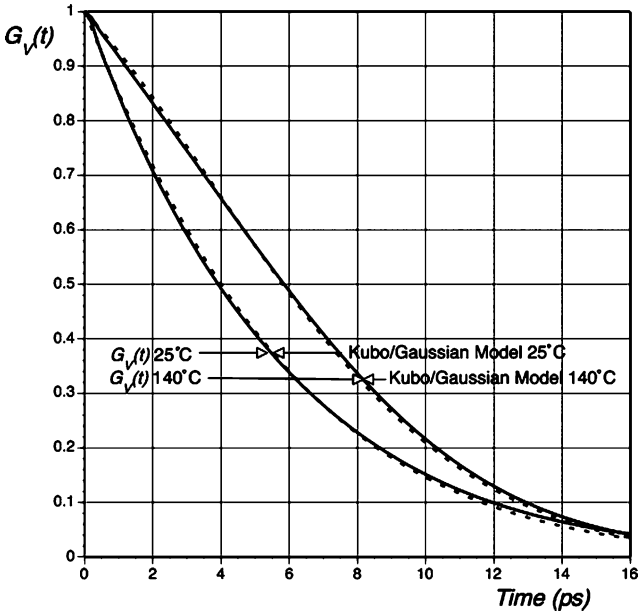

Figure 5. Plot of the time correlation functions calculated for the 1583 cm^{-1} band of *a*-PS from spectroscopic data obtained at 25 and 140 °C. Also shown are curves calculated using the Kubo model modified to account for inhomogeneous broadening.

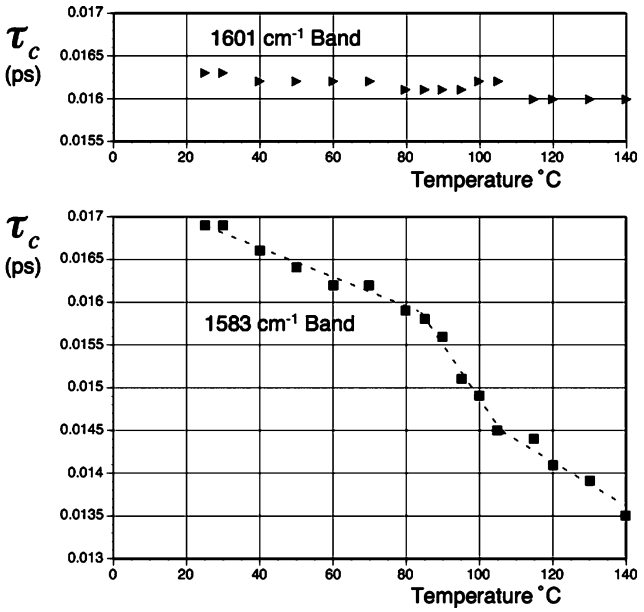

Figure 6. Plot of the correlation time, τ_c, calculated for the 1601 and 1583 cm^{-1} bands of *a*-PS as a function of temperature. The lines have been placed only as a guide to the eye.

The values of τ_c for both modes, in the range 0.01−0.02 ps, are considerably faster than values of τ_c obtained for liquids like chloroform (τ_c for the ν_3 mode ∼0.18 ps[12]) but are of the same order of magnitude as a fast relaxation process observed in acetic acid[41] and some aqueous thiocyanate solutions.[42] A high-frequency vibrational mode can relax by transferring energy to a combination of lower frequency internal and lattice or bath modes through anharmonic coupling.[43] The normal modes of *a*-PS, with its large number of internal vibrations, would therefore be expected to display fast relaxation. This ability to descend a "ladder of vibrational energy" is particularly transparent for the 1583 cm^{-1} band, with its proximity to a close-lying combination mode that has the correct symmetry for Fermi resonance interactions. In this regard, Tiller[44] calculated the dipole autocorrelation function of polystyrene in order to identify

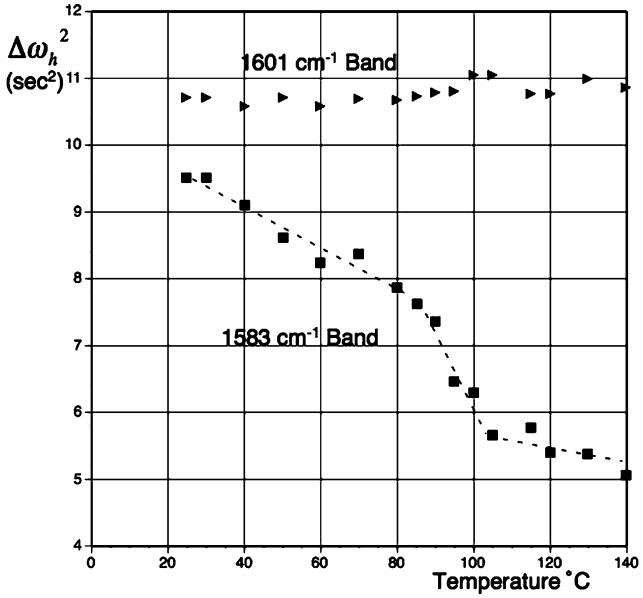

Figure 7. Plot of the contribution of homogeneous broadening to the second moment of the band profile for the 1601 and 1583 cm^{-1} bands of *a*-PS as a function of temperature. The lines have been placed only as a guide to the eye.

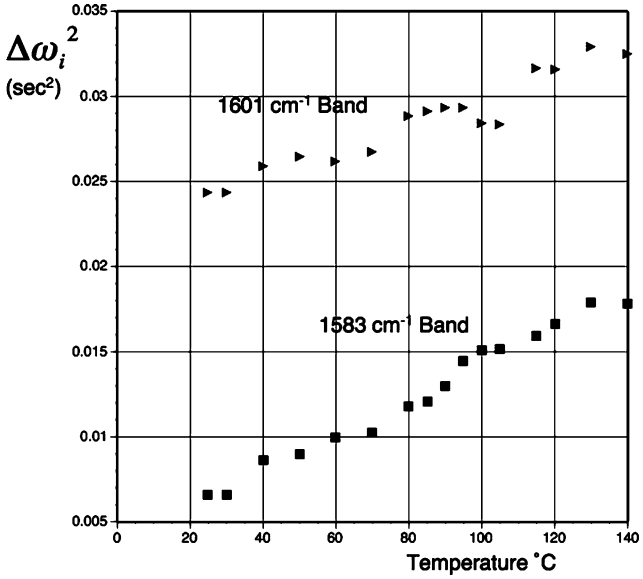

Figure 8. Plot of the contribution of inhomogeneous broadening to the second moment of the band profile for the 1601 and 1583 cm^{-1} bands of *a*-PS as a function of temperature.

the characteristic motions that are important in dielectric relaxation. In addition to the motions occurring at frequencies below 120 cm^{-1}, which was the main concern of the study, large-scale motions were observed in the range 500−700 cm^{-1}, corresponding to relaxations in the 0.01 ps time range. A particularly strong motion was calculated near 650 cm^{-1}. In our preceding paper,[6] we observed that a mode near 1593 cm^{-1} that appears to couple with and provide a mode of relaxation for the 1583 cm^{-1} band is most likely a combination of the modes observed near 906 and 698 cm^{-1}. This would suggest that energy transfer to lower frequency modes is the origin of this fast relaxation. However, fast vibrational dephasing is also a possibility. It can be seen from Figure 6 that the correlation time, τ_c, decreases with increasing temperature, indicating that the speed of modulation increases. This is also what would be expected if the fast component of the correlation decay largely reflected vibrational dephasing as a result of the subpicosecond

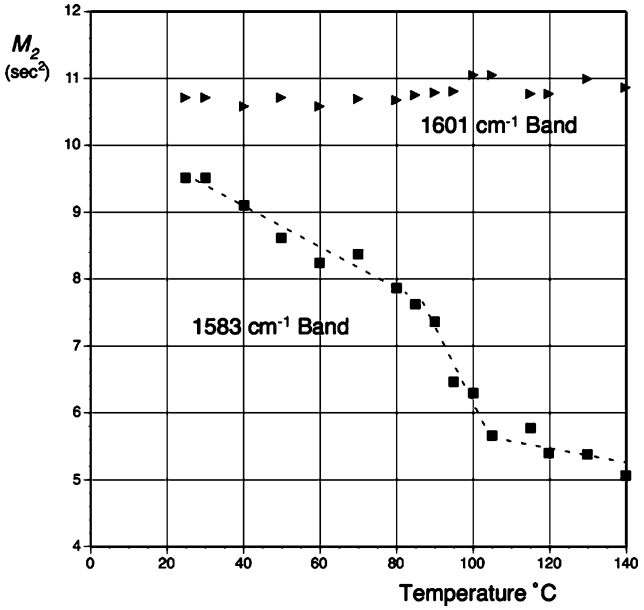

Figure 9. Plot of the second moment of the band profile for the 1601 and 1583 cm^{-1} bands of *a*-PS as a function of temperature. The lines have been placed only as a guide to the eye.

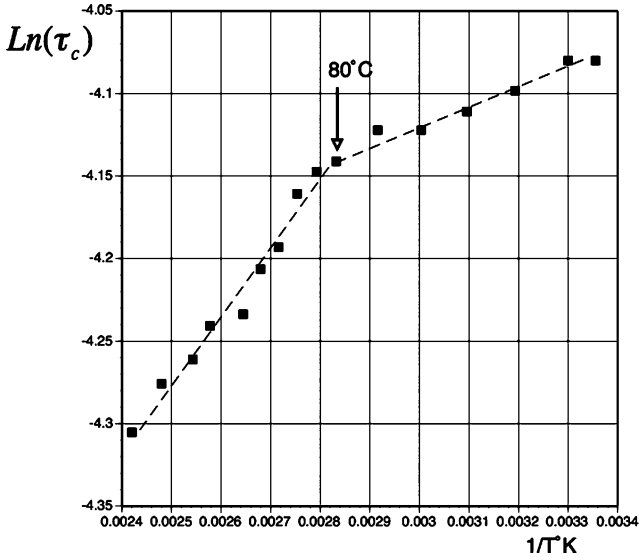

Figure 10. Plot of the log of the correlation time for the 1583 cm^{-1} band as a function of $1/T$ (K^{-1}). The lines were determined by a least-squares fit.

motions calculated by Tiller. The analysis of band shapes does not allow a distinction between these mechanisms, and it is entirely possible that both are occurring.

Figures 7 and 8 show the contribution of homogeneous and inhomogeneous broadening ($\Delta\omega_h^2$ and $\Delta\omega_i^2$) to the experimental second moment of each band. The temperature variation of M_2 is shown in Figure 9. It can be seen that the major contribution to the observed second moment comes from homogeneous broadening and thus reflects the distribution of local environments at $t \approx 0$ (i.e., static inhomogeneous broadening). At 25 °C, the values of both M_2 and $\Delta\omega_h^2$ are similar for the 1601 and 1583 cm^{-1} bands. This is not surprising, in that both are in-plane ring breathing modes, and one would expect them to be equally influenced by variations in local environment. But, as with τ_c, M_2 and $\Delta\omega_h^2$ for the 1601 cm^{-1} band vary only a little with temperature, while the second moment of the 1583 cm^{-1} band decreases significantly, with the largest rate of change seen in the 80−100 °C range. This indicates that a faster modulation process and a rapid "loss of memory" average out the effect of local differences in environment on the 1583 cm^{-1} mode.

We were surprised to find that only small values of $\Delta\omega_i^2$ were sufficient to give the relatively large deviations of $G_V(t)$ from the Kubo model. In other words, static inhomogeneous broadening, reflecting the distribution of environments that exists at the moment of excitation ($t \approx 0$), largely determines M_2. However, unlike the variation of M_2 and $\Delta\omega_h^2$ with temperature, inhomogeneous broadening, as measured by $\Delta\omega_i^2$, appears to increase steadily with temperature (Figure 8) for both the 1601 and 1583 cm^{-1} modes.

Although these data do not allow us to unambiguously assign a relaxation mechanism to these modes, the observed variations of the 1583 cm^{-1} band with temperature is interesting and consistent with contemporary views of dynamical heterogeneities in glassy systems. In an investigation of polystyrene, Roe[45] observed that the short-time dynamics consists of two processes: a fast relaxation (<1 ps) at low temperatures and a slower process (>1 ps) that is frozen in the glassy state. We calculated a correlation function that has a fast component that results in homogeneous broadening, where $\Delta\omega_h^2$ reflects the variation of the environments of the segments, each found in a "cage" of its neighbors. As the temperature is raised, a slower process, inhomogeneous broadening, increasingly affects the band profile. This is probably due to a number of factors. For the 1583 cm^{-1} band, anharmonic coupling to lower frequency modes would lead to a random modulation of this high-frequency mode and hence some degree of inhomogeneous broadening. In addition, there is now considerable evidence that glassy systems are dynamically heterogeneous,[46−48] and inhomogeneous broadening could then occur as a result of slow transitions between domains of different mobility. This would affect both the 1601 and 1583 cm^{-1} modes.

Interestingly, if motional heterogeneity is one origin of inhomogeneous broadening, it is apparent at 25 °C, the lowest temperatures where measurements were made in this study and well below the thermally observed T_g (∼100 °C). In this regard, Kanaya et al.[49] have observed a fast process in a quasi-elastic neutron scattering study of *a*-PS that had an onset temperature near 170 K. Although this relaxation is of the order of picoseconds and hence much slower than that observed here, it was assigned to librational motions of the phenyl rings. These motions are presumably as heterogeneous as other dynamic processes and would therefore lead to a degree of inhomogeneous broadening that should be observed at temperatures well below the T_g. Clearly, a number of factors, many probably related, could lead to inhomogeneous broadening, but if these were all relatively slow processes (in terms of vibrational relaxations), then their only contribution to the band profile would be through a Gaussian inhomogeneous broadening of the band. This would explain why eqs 7−10 give such a good fit to the data.

Finally, we also plotted ln τ_c against $1/T$ (K^{-1}), as shown in Figure 10. There are apparently two linear regions: one below a temperature of 80 °C and the second lying above this temperature. We assumed a temperature dependence of the following form:

$$\tau_c = \tau_0 \exp(\Delta E/kT) \tag{12}$$

In this equation, ΔE is an activation energy for the system relaxation time, τ_c. We then calculate values of ΔE of 230 cal/mol for temperatures below 80 °C and 810 cal/mol at higher

temperatures. At first glance, it is somewhat surprising that there is a larger energy barrier to relaxation at higher temperatures. However, the "fast" process observed by Kanaya et al.[49] involved only librational motions of the phenyl ring of *a*-PS at temperatures well below the T_g. Near the T_g, however, this libration becomes coupled to chain motion. There are a number of other studies that also show that larger scale ring oscillations and "flips" require cooperative motions of the ring and backbone (e.g., see ref 50 and citations therein). These occur more frequently as the T_g is approached from lower temperatures but would have a higher energy barrier.

Conclusions

Vibrational time correlation functions as a function of temperature have been calculated for the ring breathing modes observed near 1601 and 1583 cm^{-1} in the infrared spectra of *a*-PS. The correlation functions can be fit to a simple model where there is a fast relaxation process, approximated by a single relaxation time, which is inhomogeneously broadened by much slower processes. Although a number of factors can (and probably do) contribute to this inhomogeneous broadening, as long as these are all relatively slow processes (in terms of vibrational relaxations), then their only contribution to the band profile would be through a Gaussian term. Plots of relaxation times and band moments for the 1583 cm^{-1} mode as a function of temperature display changes in slope near 80 °C, about 20 °C below the thermally measured T_g. This band is more sensitive to temperature than the mode near 1601 cm^{-1} as a result of coupling to low-frequency modes through a Fermi resonance interaction with a close-lying combination mode.

Acknowledgment. The authors gratefully acknowledge the support of the National Science Foundation, Polymers Program, under Grant DMR-0551465, and the Korea Research Foundation (KRF-2003-013-D00023).

References and Notes

(1) Hannon, M. J.; Koenig, J. L. *J. Polym. Sci., Part A-2* **1969**, *7*, 1085.
(2) Huang, Y. S.; Koenig, J. L. *J. Appl. Polym. Sci.* **1971**, *15*, 1237.
(3) Ogura, K.; Kawamura, S.; Sobue, H. *Macromolecules* **1971**, *4*, 79.
(4) Ogura, K. *Br. Polym. J.* **1975**, *7*, 221.
(5) Tashiro, K.; Yoshioka, A. *Macromolecules* **2002**, *35*, 410.
(6) Painter, P. C.; Sobkowiak, M.; Park, Y. *Macromolecules* **2007**, *40*, 1730.
(7) Doge, G.; Yarwood, J. In *Spectroscopy and Relaxation of Molecular Liquids*; Steele, D., Yarwood, J., Eds.; Elsevier: Amsterdam, 1991; Chapter 6.
(8) Rothschild, W. D. *Dynamics of Molecular Liquids*; John Wiley & Sons: New York, 1984.
(9) Oxtoby, D. W. *Adv. Chem. Phys.* **1979**, *40*, 1.
(10) Kirillov, S. A. *J. Mol. Liq.* **1998**, *76*, 35.
(11) Rothschild, W. G. *J. Phys. Chem.* **1976**, *65*, 455.
(12) Rothschild, W. G.; Cavagnat, R. M. *J. Chem. Phys.* **1992**, *97*, 2900.
(13) Cataliotti, R. S.; Foggi, P.; Giorgini, M. G.; Mariani, L.; Morresi, A.; Paliani, G. *J. Chem. Phys.* **1993**, *98*, 4372.
(14) Navarro, R.; Bratu, I.; Henanz, A. *J. Phys. Chem.* **1993**, *97*, 9081.
(15) Yi, J.; Jonas, J. *J. Phys. Chem.* **1996**, *100*, 16789.
(16) Stolov, A. A.; Herrebout, W. A.; van der Veken, B. J.; Remizov, A. B. *J. Phys. Chem. B* **1998**, *102*, 6493.
(17) Kirillov, S. A.; Yannopoulos, S. N. *J. Chem. Phys.* **2002**, *117*, 1220.
(18) Kirillov, S. A.; Voyiatzis, I. S.; Musiyenko, G. M.; Photiadis, G. M.; Pavlatou, E. A. *J. Chem. Phys.* **2001**, *114*, 3683.
(19) Kalampounias, A. G.; Yannopoulos, S. N.; Steffen, W.; Kirillova, L. I.; Kirillov, S. A. *J. Chem. Phys.* **2003**, *118*, 8340.
(20) Perrot, M.; Rothschild, W. G.; Cavagnat, R. M. *J. Chem. Phys.* **1999**, *110*, 9230.
(21) Oxtoby, D. W. *J. Chem. Phys.* **1981**, *74*, 1503.
(22) Mariani, L.; Moressi, A.; Cataliotti, R. S.; Giorgini, M. G. *J. Chem. Phys.* **1996**, *104*, 914.
(23) Kirillov, S. A. *Chem. Phys. Lett.* **1999**, *303*, 37.
(24) Snyder, R. G.; Maroncelli, M.; Strauss, H. L.; Hallmark, V. M. *J. Phys. Chem.* **1986**, *90*, 5623.
(25) Lau, C. La; Snyder, R. G. *Spectrochim. Acta* **1971**, *27A*, 2073.
(26) Painter, P. C.; Koenig, J. L. *J. Polym. Sci., Polym. Phys. Ed.* **1977**, *15*, 1885.
(27) Snyder, R. G.; Painter, P. C. *Polymer* **1981**, *22*, 1633.
(28) Musso, M; Torii, H.; Giorgini, M. G.; Doge, G. *J. Chem. Phys.* **1999**, *110*, 10076.
(29) Painter, P. C.; Pehlert, G. J.; Hu, Y.; Coleman, M. M. *Macromolecules* **1999**, *32*, 2055.
(30) Kubo, R. In *Fluctuations, Relaxation and Resonance in Magnetic Systems*; ter Haar, G., Ed.; Plenum: New York, 1962.
(31) Lauberau, A.; Wochner, G.; Kaiser, W. *Chem. Phys.* **1978**, *28*, 363.
(32) Harris, C. B.; Autweter, H.; George, S. M. *Phys. Rev. Lett.* **1980**, *44*, 737.
(33) George, S. M.; Auweter, H.; Harris, C. B. *J. Chem. Phys.* **1980**, *73*, 5573.
(34) Oxtoby, D. W. *J. Chem. Phys.* **1981**, *74*, 5371.
(35) Kato, T. *J. Chem. Phys.* **1986**, *84*, 3409.
(36) Loring, R. F.; Mukamel, S. *J. Chem. Phys.* **1985**, *83*, 2116.
(37) Goodyear, G.; Tucker, S. C. *J. Chem. Phys.* **1999**, *111*, 9673.
(38) Graf, R. T.; Koenig, J. L.; Ishida, H. *Appl. Spectrosc.* **1985**, *39*, 405.
(39) Giorgini, M. G.; Arcioni, A.; Polizzi, C.; Musso, M.; Ottaviani, P. *J. Chem. Phys.* **2004**, *120*, 4969.
(40) Liu, Y.; Lin, J.; Huang, G.; Guo, Y.; Duan, C. *J. Opt. Soc. Am.* **2001**, *B 18*, 666.
(41) Lim, M.; Hochstrasser, R. M. *J. Chem. Phys.* **2001**, *115*, 7629.
(42) Kato, T. *J. Chem. Phys.* **1983**, *79*, 2139.
(43) Kenkre, V. M.; Tokmakoff, A.; Fayer, M. D. *J. Chem. Phys.* **1994**, *101*, 10618.
(44) Tiller, A. R. *Macromolecules* **1992**, *25*, 4605.
(45) Roe, R. J. *J. Non-Cryst. Solids* **1998**, *235*−*237*, 308.
(46) Sillescu, H. *J. Non-Cryst. Solids* **1999**, *243*, 81.
(47) Ediger, M. D. *Annu. Rev. Phys. Chem.* **2000**, *51*, 99.
(48) Garrahan, J. P.; Chandler, D. *Phys. Rev. Lett.* **2002**, *89*, 35704.
(49) Kanaya, T.; Kawaguchi, T.; Kaji, K. *J. Chem. Phys.* **1996**, *104*, 3841.
(50) Lyulin, A. V.; Michels, M. A. J. *Macromolecules* **2002**, *35*, 1463.

MA062423C